SAN FRANCISCO BAY NUTRIENT MANAGEMENT STRATEGY

Continuous Suspended Sediment Monitoring in South and Lower South San Francisco Bay

Final Report

Martin Volaric
Lilia Mourier
Lucy Montgomery
Katie Noland
David Senn
Ariella Chelsky

[1]San Francisco Estuary Institute

May 2025

SFEI Contribution #1229

Executive Summary

This report presents results from a three-year effort (2022-2024) to estimate continuous suspended sediment concentration (SSC) in the South Bay (SB) and Lower South Bay (LSB) subembayments of San Francisco Bay (SFB). We used discrete SSC samples to calibrate high-frequency (15-min) turbidity measurements from the Nutrient Management Strategy's (NMS) moored sensor array, resulting in high-frequency SSC estimates at eight study sites. This effort represents a collaboration between the NMS, San Francisco Bay Regional Monitoring Program, and South Bay Salt Pond Restoration Project.

The moored sensor array used for turbidity data collection consisted of 7 YSI EXO2 multiparameter sondes and 1 PME C7 turbidity-only sensor. We evaluated several turbidity-SSC models for the 7 EXO2 sites, ultimately selecting a series of three slope-only (y-intercept = 0) least squares linear regressions (LSLRs) from $\log_{10}$-$\log_{10}$ transformed data grouped together based on the three habitat types in SB and LSB (channel, slough, and shoal). This calibration model represents a change from Year 1 and Year 2 reports, which utilized a linear mixed effect model (LMM). Turbidity from the C7 site was also calibrated using a slope-only LSLR from $\log_{10}$-$\log_{10}$ data. Calibrations at all sites showed reasonable agreement between $\log_{10}$(turb) and $\log_{10}$(SSC), with R^2 = 0.89, 0.87, and 0.85 for regressions at the channel, slough, and shoal sites, respectively, and R^2 = 0.93 for the C7 site. From these calibrations we created continuous 15-min SSC datasets at 8 locations, representing 1 channel, 4 shoal, and 3 slough sites. These high-frequency SSC data are designed for use in more targeted studies of SFB SSC dynamics, and will be made available for download from the San Francisco Estuary Institute (SFEI) website.

Suggested citation:
Volaric, M; Mourier, L.; Montgomery, L.; Noland, K.; Senn, D.; Chelsky, A. 2025. Continuous Suspended Sediment Monitoring in South and Lower South San Francisco Bay: Final Report. SFEI Contribution No. 1229. San Francisco Estuary Institute: Richmond, CA.

Acknowledgments

This work was funded by the South Bay Salt Pond Restoration Project, the Regional Monitoring Program for Water Quality in San Francisco Bay, and the San Francisco Bay Nutrient Management Strategy. We thank staff from USGS PCMSC Marine Facility and USGS California Water Science Center for field support, and D Hart and R Allen from the USGS for providing feedback on selecting the final calibration model. We also thank the following Watershed Stewards Program corpsmembers for assisting with fieldwork: L Partida, C Diamant, and O Hockley-Rodes.

List of Acronyms

Abbreviation	Meaning
a	Slope parameter of best fit model
ALV	Alviso Slough mooring
b	Y-intercept of best fit model
BCF	Bias correction factor for $\log_{10}$ transformed data
C7, PME C7	Turbidity-only sensor
CIMIS	California Irrigation Management Information System
DMB	Dumbarton Bridge mooring
EDL	Eden Landing Whale's Tail mooring
EXO2, YSI EXO2	Multiparameter water quality sensor
FE	LMM fixed effects
FNU	Formazin Nephelometric Units (turbidity)
GL	Guadalupe Slough mooring
HAY	Hayward mooring
HCEP	Seabird Hydrocat multiparameter sensor
LMM	Linear Mixed Effect Model
LSB	Lower South San Francisco Bay
LSLR	Least Squares Linear Regression
MSP	Moored Sensor Program
NMS	Nutrient Management Strategy
NTU	Nephelometric Turbidity Units
NW	Newark Slough mooring
QA/QC	Quality assurance and quality control
RBR solo	Wave sensor
RE	LMM random effects
RMP	Regional Monitoring Program
SB	South San Francisco Bay
SBSPRP	South Bay Salt Pond Restoration Project
SFB	San Francisco Bay
SFEI	San Francisco Estuary Institute
SHL	Shoal mooring
SLM	San Leandro Marina mooring
SM	San Mateo Bridge mooring
SMP	Sediment Monitoring Program
SSC	Suspended Sediment Concentration
USGS	United States Geological Survey

1. Introduction

Spatiotemporal variance of suspended sediment concentration (SSC) in San Francisco Bay (SFB) is of key interest to regional water quality, wetland, and fisheries managers. Accurate measurements of SSC are critical for quantifying sediment delivery to shorelines, migration of particle-associated contaminants, light attenuation for phytoplankton growth, and habitat suitability for marine wildlife (Cloern 1987, Cloern and Jassby 2012, Newcombre and Jensen 1996). SSC and sediment transport processes are especially relevant to the South Bay (SB) and Lower South Bay (LSB) subembayments of SFB due to historical mercury loading, significant nutrient enrichment from publicly owned treatment works (POTWs), and adjacent large-scale marsh and wetland restoration projects around the Bay's perimeter (Marvin-DiPasquale et al. 2022, SFEI 2016, Shellenbarger et al. 2013, Valoppi 2018). Currently, the only publicly available continuous SSC data for SB and LSB are from a United States Geologic Survey (USGS) monitoring site in the deep channel off the Dumbarton Bridge, although summaries of USGS SSC monitoring efforts at other stations for specific water years are described in numerous public reports (e.g., Livsey et al. 2020). With ongoing SSC monitoring limited to the deep channel, a critical gap exists for shallow margin shoal and slough habitats in SB and LSB.

To address the SSC monitoring gap for SFB, a collaboration was formed between the San Francisco Bay Nutrient Management Strategy (NMS), Regional Monitoring Program (RMP), and South Bay Salt Pond Restoration Project (SBSPRP), to expand SSC data collection in the region through the creation of the Sediment Monitoring Program (SMP). Continuous estimates of SSC are difficult, and are often achieved through calibration of *in situ* turbidity sensor measurements with discrete SSC grab samples (Rasmussen et al. 2009). As part of its role monitoring water quality within SFB, the NMS manages an array of high frequency (15-min) multiparameter sondes (YSI EXO2) that record a suite of environmental data throughout SB and LSB, including turbidity. The goal of this project was to augment the turbidity data at 7 NMS sites with discrete SSC samples in order to formulate a turbidity-SSC calibration for SB. This project also established an eighth turbidity monitoring station using a turbidity-only sensor (PME C7), with accompanying discrete SSC sample collection, and deployed a wave gauge (RBR solo) on the eastern SB shoal (Hayward site) to better understand the impacts of waves on SSC dynamics.

Several mathematical models can be used to define a turbidity-SSC relationship, with the most common being least-squares linear regression (LSLR). There are several ways to apply LSLR, including both with and without a vertical offset (y-intercept), $\log_{10}$-$\log_{10}$ transformation, or additional independent variables such as dissolved organic matter or chlorophyll concentration. The presence/absence of a y-intercept is particularly relevant for SSC calibrations. Conceptually, SSC must be equal to zero when there is no turbidity, so the presence of a y-estimate is likely to overestimate SSC when turbidity is low. LSLRs are simple to apply, and are the approach typically favored by the USGS (Rasmussen et al. 2009). For the Year 1 and Year 2 SMP reports (Mourier et al. 2023, Mourier et al. 2024) we applied a linear mixed effect model (LMM) in lieu of an LSLR to the 7 EXO2 sites. LMMs are useful when relationships between dependent and independent variables are likely to be similar among different groups, such as between turbidity and SSC across moored sensor locations. However, LMMs are much more complicated than LSLRs, and may fail to converge when there are limited differences between groups.

In this report, we discuss the methodology for creating our final turbidity-SSC calibration for SFB. We compare the results from 3 calibration models: a set of 3 LSLRs with data grouped by the primary habitats of SB and LSB (slough, channel, shoal) (Model #1), site-specific LSLRs (Model #2), and a LMM (Model #3). Model 1 and Model 2 were tested both with and without a y-intercept, while all three models were evaluated both with untransformed and with $\log_{10}$-$\log_{10}$ transformed data. We also

describe general patterns of turbidity and SSC dynamics in SFB, including results from the wave gauge at the Hayward station, with this report focused on the period 2022-2024. The final calibration model was used to create continuous SSC datasets for all 8 monitoring locations, which stretch back as far as 2013 at some sites. These SSC data will be made available for download from the San Francisco Estuary Institute's (SFEI's) website.

2. Methods

2.1 Data collection

2.1.1 Study sites and turbidity monitoring

The NMS collects high-frequency (15-min) water quality data at several locations throughout SFB using YSI EXO2 multiparameter sondes as part of its Moored Sensor Program (MSP). Turbidity data from 7 of these sites (Figure 1) were calibrated for SSC: San Mateo Bridge (SM), San Leandro Marina (SLM), Hayward (HAY), Shoal (SHL), Newark Slough (NW), Guadalupe Slough (GL), and Alviso Slough (ALV). As part of this effort, an additional PME C7 turbidity sensor was deployed on the SB shoal offshore of the Eden Landing Whale's Tail (EDL). Of these 8 total stations, one is in the SB deep channel (SM), four are located on the SB shoal (SLM, HAY, SHL, EDL), and three are in LSB sloughs (NW, GL, ALV) (Figure 1, Table 1). Turbidity data at these sites stretches back as far as Sep 2013 (Table 1). Turbidity at SM was recorded with a Seabird HydroCat prior to August 2022, and with an EXO2 from August 2022-present. The EXO2s record turbidity using Formazin Nephelometric Units (FNU), while the C7 and HydroCat measure in Nephelometric Turbidity Units (NTU).

Turbidity stations were serviced every 3-5 weeks. During each servicing trip, instruments were either swapped for lab-cleaned and calibrated instruments, or field-serviced through cleaning, calibration checks, and battery replacement. Following retrieval, we ran all data through a multistep quality assurance and quality control (QA/QC) process in accordance with MSP procedures to remove erroneous data. Please note that the C7 turbidity sensor at EDL was only deployed for roughly half of the project duration due to a malfunction requiring manufacturer repair, followed by later removal to prevent damage from a USGS sediment deposition and transport study in the area.

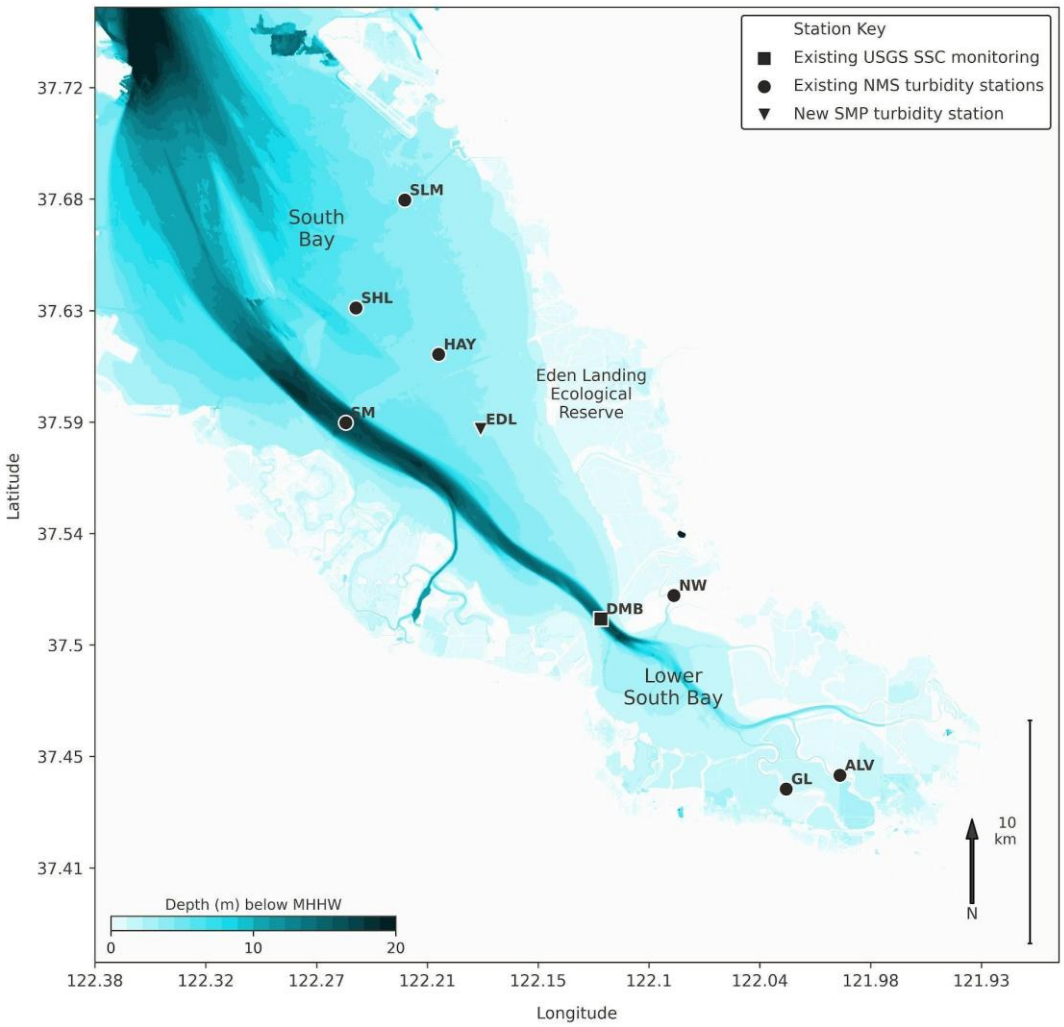

Figure 1. Map of South San Francisco Bay turbidity monitoring stations. Station names are presented in Table 1 below.

Table 1. Summary of turbidity monitoring stations depicted in Figure 1.

Station	Lat	Long	Dist above bed (m)	Date installed	Habitat type	Equipment
San Mateo Bridge (SM)	37.584	-122.25	10	July 2014	Channel	EXO2, HCEP
San Leandro Marina (SLM)	37.674	-122.22	1.3	Nov 2020	Shoal	EXO2
Hayward (HAY)	37.611	-122.2	1	Oct 2020	Shoal	EXO2, RBR
Shoal (SHL)	37.63	-122.24	0.8	Aug 2020	Shoal	EXO2
Eden Landing (EDL)	37.581	-122.18	0.5	Jan 2020	Shoal	C7
Newark Slough (NW)	37.513	-122.08	1.3	April 2015	Slough	EXO2
Guadalupe Slough (GL)	37.435	-122.03	0.5	June 2015	Slough	EXO2
Alviso Slough (ALV)	37.44	-122	0.5	Sep 2013	Slough	EXO2

2.1.2 Discrete sample collection

Discrete SSC samples were collected every 3-5 weeks at each site. As part of the NMS MSP, discrete SSC samples have been collected at SM, SLM, HAY, and SHL since 2020. Beginning January 2022, monthly discrete SSC sampling was expanded to EDL, NW, GL, and ALV. SSC samples were collected at the approximate instrument depth (± 1 m) following standard USGS procedures (Rasmussen et al. 2009). At SM, SLM, HAY, and SHL, samples were collected using a submersible centrifugal pump while EDL, NW, GL, and ALV samples were collected using a Van Dorn sampler. Discrete samples were analyzed for total sediment concentration and percent fines at the USGS Santa Cruz Sediments Laboratory, with total sediment concentration used in the calibration models.

2.1.3 Wave monitoring

To better understand turbidity and SSC dynamics in the SFB, wave characteristics were measured at the HAY station using an RBR solo high-frequency wave sensor. As with the turbidity sondes, the wave sensor was serviced every 3-5 weeks. During each servicing trip the wave sensor was cleaned, data were offloaded and reviewed, and the battery was replaced. Using the sensor-specific program Ruskin, we calculated significant wave height and period, 90th percentile wave height and period, maximum wave height and period, and average wave height and period. All values were calculated at 5 min resolution from 4 Hz pressure data. Results were processed through a multi-level QA/QC procedure that included statistical filtering and manual review to remove erroneous data. In total we recorded ~18 months of near-continuous wave data. These were paired with turbidity data and SSC results from the HAY EXO2 to better understand the impact of waves on sediment dynamics on the SB shoal.

2.2 Calibration model development

We tested three turbidity-SSC calibration models for the EXO2 sites. These were: 1) a set of 3 LSLRs with data grouped into the 3 SB habitat types (channel, shoal, slough), 2) a set of 7 site-specific LSLRs, and 3) a LMM. As EDL utilized a PME C7 turbidity sensor rather than an EXO2, LSLR was always used for calibration at this site. Additionally, since SM turbidity data prior to August 2022 was recorded using a Seabird HydroCat rather than an EXO2, only data from after August 2022 was used for calibration. Turbidity values used for calibration were defined as the mean of measurements taken $\pm$ 20 min around the time of discrete SSC sample collection, ensuring 2-3 turbidity data points were used for each SSC calibration point. All models were evaluated both with linear (untransformed) and $\log_{10}$-$\log_{10}$ transformed data. Models 1 and 2 were tested both with and without y-intercepts. The LMM (Model 3) failed to converge when the y-intercept was removed, so only a model with an intercept was considered.

2.2.1 Calibration Models 1 and 2: Least squares linear regression (LSLR)

Calibration models (1) and (2) utilized least squares linear regression (LSLR). An LSLR with untransformed data takes the form:

$$SSC = a * turb + b \quad (1)$$

With $\log_{10}$-$\log_{10}$ transformation this equation becomes:

$$log_{10}(SSC) = a * log_{10}(turb) + b \quad (2)$$

In both Eq. (1) and Eq. (2) a is the slope and b the y-intercept.

With the y-intercepts (b) removed, these equations become:

$$SSC = a * turb \text{ and } log_{10}(SSC) = a * log_{10}(turb) \quad (3,4)$$

Habitat-specific LSLRs were grouped as follows: channel – SM; shoal – SHL, HAY, SLM; slough – ALV, GL, NW.

2.2.2 Calibration Model 3: Linear mixed effect model (LMM)

LMMs combine fixed effects (FE) shared across all sites with site-specific random effects (RE). For our turbidity-SSC calibration model, the LMM for each site takes the form:

$$SSC = (a_{FE} + a_{RE}) * turb + (b_{FE} + b_{RE}) \quad (5)$$

or $$log_{10}(SSC) = (a_{FE} + a_{RE}) * log_{10}(turb) + (b_{FE} + b_{RE}) \quad (6)$$

where a_{FE} and a_{RE} are the fixed and random effects slopes, respectively, and b_{FE} and b_{RE} are the fixed and random effects y-intercepts. As with the LSLR, the presence of a y-intercept is likely to overestimate SSC when turbidity is low. However, when removing the y-intercept the model failed to converge. As a LMM with y-intercepts was the model used for the Year 1 and Year 2 reports (Mourier et al. 2023, Mourier et al. 2024), we evaluated this model primarily for comparison to Model 1 and Model 2 described above.

2.2.3 Bias Correction Factor (BCF) for log_{10}-log_{10} model results

Results from log_{10}-log_{10} models must be retransformed to their original units (i.e., 10 raised to the power of the model results) to estimate SSC. This retransformation step often introduces a negative bias to SSC estimates, particularly when correlations are relatively weak (Rasmussen et al. 2009). In order to correct for this error, we calculated the bias correction factor (BCF) as described by Rasmussen et al. (2009). The BCF is defined as:

$$BCF = \frac{\sum_{i=1}^{n} 10^{e_1}}{n} \quad (7)$$

where n is the number of discrete SSC samples and e_1 is the residual SSC in log_{10} units. SSC results were corrected for bias by multiplying the retransformed values by the BCF.

2.2.4 Turbidity thresholds used for SSC calibration

USGS standard methodology suggests that SSC estimates are not reliable when turbidity is > 110% of the maximum value used during calibration (Rasmussen et al. 2009). We therefore constrained habitat-specific and site-specific LSLRs by the turbidity used for calibration at each habitat or site, respectively, while for the LMM the greatest turbidity calibration value from any site was the threshold for all sites. For this report and accompanying dataset, we flagged SSC results calculated when turbidity was above this 110% threshold. Although SSC data were calculated for all turbidity measurements, including those above this threshold, please note that SSC calculated from out of range turbidity values should be treated with caution.

3. Results

3.1 Turbidity and discrete SSC data

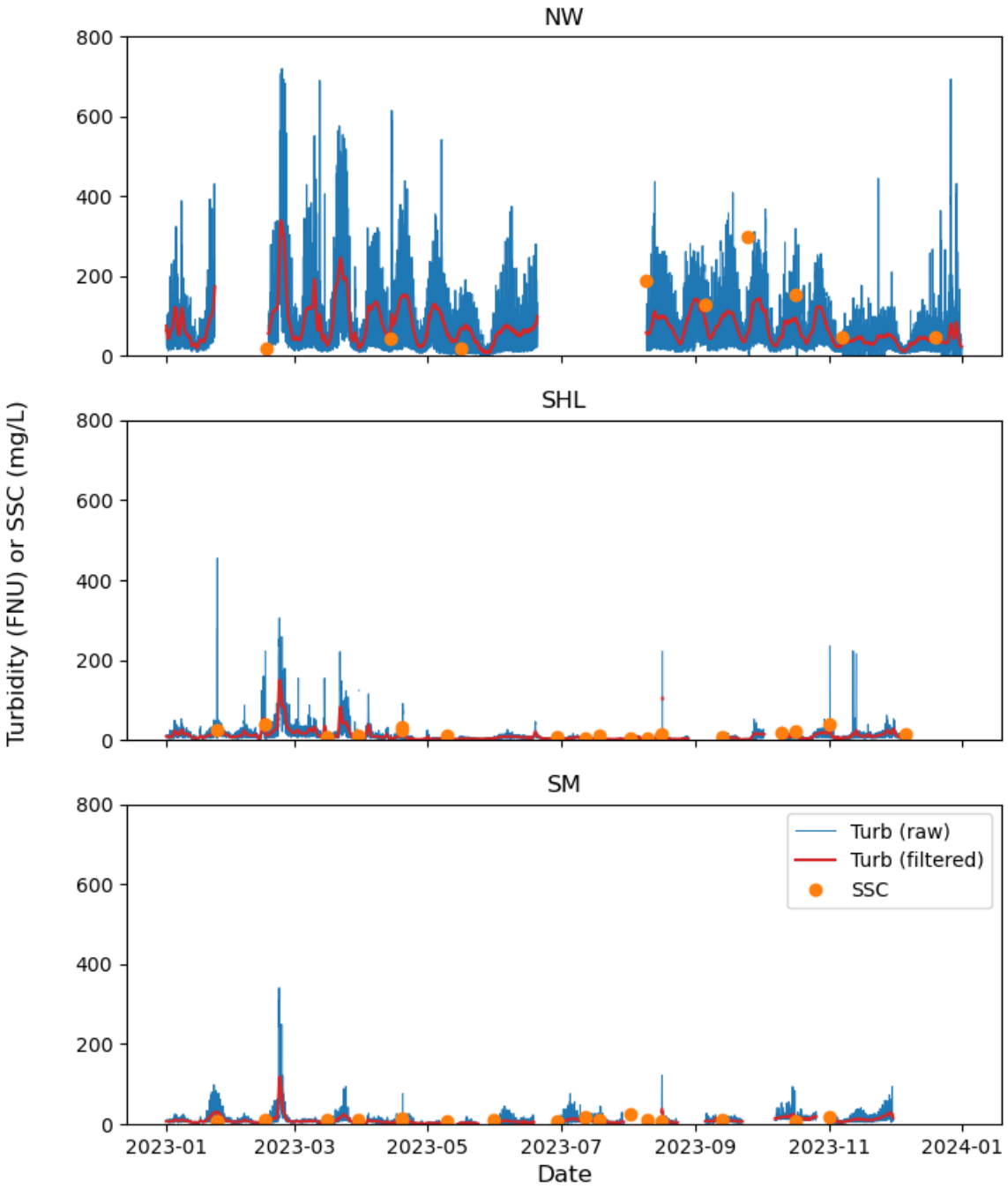

Figure 2. Discrete SSC and tidally filtered turbidity data from representative sites of the three habitat types (slough - NW, shoal - SHL, channel - SM) from January 2023 to January 2024.

Turbidity results for this study are for Jan 2022-Oct 2024, although turbidity data and SSC grab samples used for calibration stretch back as far as 2020 (see below). In general, turbidity tended to be greater and more variable at the slough sites (ALV, GL, NW) than at the channel (SM) or shoal (SHL, HAY, SLM,

EDL) stations. Tidally filtered turbidity ranged from ~50-250 FNU in the sloughs while tending to remain < 50 FNU on the shoal and in the channel (Figure 2). Turbidity remained relatively consistent throughout the year at both slough and channel stations, while values at the shoal stations tended to be slightly elevated in springtime compared to the rest of the year. Mean unfiltered turbidity for the duration of the study period across sites ranged from 28 to 53 FNU at the slough stations and 10 to 22 FNU/NTU at the channel and shoal stations (Table 2).

Table 2. Turbidity statistics from 15-min continuous dataset collected during the study period (2022-2024) in either FNU (ALV, GL, NW, SM, HAY, SHL, SLM) or NTU (EDL).

Station	Mean	SD	$P25^{th}$	$P50^{th}$	$P75^{th}$
Alviso Slough (ALV)	28	24	13	21	38
Guadalupe Slough (GL)	51	41	24	44	74
Newark Slough (NW)	53	51	17	42	70
San Mateo Bridge (SM)	11	14	4	6	11
Hayward (HAY)	12	14	4	6	12
Shoal (SHL)	10	9	4	9	15
San Leandro Marina (SLM)	16	23	3	11	23
Eden Landing (EDL)	22	26	6	12	26

Consistent with turbidity data, SSC values were larger at the slough stations (mean 63-112 mg/L) than the channel/shoals (mean 22-39 mg/L) (Table 3). The total number of discrete samples for each site ranged from n=14 at EDL to n=54 at SM, where sample collection predated this study. For reference, USGS guidelines recommend n>30 discrete SSC samples per site to create robust turbidity-SSC calibrations via LSLR. This threshold was achieved at all sites except EDL.

Table 3. Discrete SSC distribution statistics. SD - standard deviation and P - percentile. Values are in mg/L.

Station	n	Mean	SD	P25th	P50th	P75th	Max
Alviso Slough (ALV)	31	63	50	33	42	70	210
Guadalupe Slough (GL)	30	112	108	50	91	115	600
Newark Slough (NW)	30	102	78	45	74	147	297
San Mateo Bridge (SM)	54	22	22	9	15	24	145
Hayward (HAY)	51	26	27	11	15	31	132
Shoal (SHL)	50	23	17	11	19	31	75
San Leandro Marina (SLM)	50	29	28	11	16	35	125
Eden Landing (EDL)	14	39	65	11	18	28	269

3.2 Calibration model results

Slope only versions of $\log_{10}$-$\log_{10}$ transformed data showed the strongest fits for Model 1 and Model 2 as judged by R^2 (Model 1 R^2 = 0.85-0.89, Model 2 R^2 = 0.84-0.90; Table 4). These R^2 were considerably higher than for slope-only untransformed models (Model 1 R^2 = 0.51-0.67, Model 2 R^2 = 0.33-0.76; Table 4). With the y-intercept included, both Model 1 and Model 2 had particularly low R^2, with low-end values of 0.00-0.09 depending on whether data was transformed (Table 4). When included, y-intercepts could be substantial, particularly at the sloughs, with values for Model 1 and Model 2 ranging from 60-

70 mg/L (Table 5, Table 6). In other words, the minimum SSC predicted by Model 1 and Model 2 are as high as 70 mg/L for some sites, which is not consistent with actual SSC values. As a result, only slope-only models were considered. As Model 3 (LMM) failed to converge when the y-intercept was removed, only Model 1 and Model 2 were evaluated in greater detail. The PME C7 sensor at EDL was calibrated separately from the 7 EXO2 sites using a site-specific calibration. Results from the EDL calibration are presented with EXO2 calibrations in Tables 4-6 below.

Best-fit coefficients were similar between Model 1 and Model 2 when comparing either slope-only versions or slope + intercept variations for both linear (Table 5) and log_{10}-log_{10} data (Table 6). For example, the untransformed slope-only parameter *a* (slope) for the slough stations in Model 1 was 1.11 (Table 5), which was in the range of *a* values when calculated individually for Model 2 (0.96-1.24). These similarities between linear Model 1 and Model 2 were consistent for shoal sites (Table 5), and for log_{10}-log_{10} transformed data (Table 6). Different habitats in Model 1 also showed similarity with one another. Slope-only *a* values were close between slough and shoal stations (1.11 vs. 1.15) when linear data was used, though the channel *a* value was somewhat higher (1.40; Table 5). With log_{10}-log_{10} data, slope-only *a* values were similar at all habitat types (1.13 - 1.18; Table 6).

Table 4. Summary Statistics from the 3 calibration models. Please note the LMM (Model 3) failed to converge when the y-intercept was removed. The package used to calculate the Model #3 LMM (statsmodels.api in Python) does not compute an R^2 value.

	Linear				LogLog			
	Slope only		With y-int		Slope only		With y-int	
Model	R^2	p	R^2	p	R^2	p	R^2	p
1. LSLR (Habitat)	0.51-0.67	<0.001	0.09-0.31	<0.001-0.06	0.85-0.89	<0.001	0.04-0.38	<0.001-0.36
2. LSLR (site)	0.33-0.76	<0.001-0.004	0.00-0.49	<0.001-0.06	0.84-0.90	<0.001	0.02-0.68	<0.001
3. LMM	-	-	-	<0.001	-	-	-	0.001
LSLR (EDL)	0.53	0.005	0.38	0.08	0.93	0.001	0.01	0.65

Table 5. Best-fit parameters for linear models fit both with and without y-intercepts (±95% CI). The parameters *a* and *b* refer to the slope and intercept, respectively, of the linear best fit relationship between SSC and turbidity. Best fit parameters for models run with log_{10}-log_{10} data are depicted in Table 6. Please note the LMM (Model 3) failed to converge when the y-intercept was removed. Fixed-effects coefficients for the LMM with y-intercept were *a*: 0.58 ± 0.26, *b*: 35.7 ± 21.4.

	Linear (untransformed)							
	1. LSLR (habitat)			2. LSLR (site)			3. LMM	
	Slope only	With y-int		Slope only	With y-int		With y-int	
Site	a	a	b	a	a	b	a	b
Alviso Slough (ALV)	1.11±0.26	0.38±0.28	66.8±18.4	0.96±0.62	0.06±0.64	65.3±32.4	0.44	54.2
Guadalupe Slough (GL)				1.24±0.45	0.44±0.50	70.9±32.8	0.40	69.1
Newark Slough (NW)				1.08±0.41	0.41±0.47	69.6±35.0	0.41	66.9
San Mateo Bridge (SM)	1.40±0.49	0.76±0.81	7.6±7.94	1.40±0.49	0.76±0.81	7.57±7.94	0.74	10.1
Hayward (HAY)	1.15±0.19	0.74±0.21	15.4±4.97	1.31±0.47	0.76±0.54	16.5±10.2	0.69	18.0
Shoal (SHL)				1.59±0.29	1.05±0.35	10.3±4.88	0.72	14.4
San Leandro Marina (SLM)				1.06±0.25	0.73±0.26	16.2±7.44	0.70	17.4
Eden Landing (EDL)	-	-	-	7.30±4.6	8.78±7.95	-15.1±64.6	-	-

Table 6. Best-fit parameters for log_{10}-log_{10} models fit both with and without y-intercepts (±95% CI). The parameters *a* and *b* refer to the slope and intercept, respectively, of the least squares best fit relationship between SSC and turbidity. Best fit parameters for models run with untransformed data are depicted in Table 5. Please note the LMM (Model 3) failed to converge when the y-intercept was removed. Fixed-effects coefficients for the LMM with y-intercept were *a*: 0.36 ± 0.21, *b*: 1.09 ± 0.28.

	Log-Log							
	1. LSLR (habitat)			2. LSLR (site)			3. LMM	
	Slope only	With y-int		Slope only	With y-int		With y-int	
Site	a	a	b	a	a	b	a	b
Alviso Slough (ALV)	1.13±0.09	0.30±.09	1.40±0.14	1.17±0.20	0.07±0.24	1.64±0.34	0.14	1.55
Guadalupe Slough (GL)				1.13±0.18	0.36±0.11	1.37±0.17	0.36	1.34
Newark Slough (NW)				1.11± 0.15	0.34±0.17	1.35±0.27	0.35	1.32
San Mateo Bridge (SM)	1.18±0.22	0.19±0.42	0.91±0.36	1.17±0.22	0.19±0.42	0.91±0.36	0.29	0.85
Hayward (HAY)	1.18±0.09	0.41±0.11	0.91±0.11	1.25±0.18	0.43±0.22	0.89±0.21	0.43	0.90
Shoal (SHL)				1.29±0.15	0.57±0.23	0.73±0.21	0.55	0.75
San Leandro Marina (SLM)				1.18±0.15	0.41±0.15	0.93±0.16	0.41	0.93
Eden Landing (EDL)	-	-	-	1.75±0.31	1.08±0.56	0.57±0.43	-	-

Residual plots were calculated for slope-only Model 1 and Model 2 for both linear (Figure 3) and log_{10}-log_{10} transformations (Figure 4). Residuals for untransformed data showed a linear pattern at several sites, with positive values at low SSC and negative values at high SSC (Figure 3). Residuals from log_{10}-log_{10} transformed models showed no obvious pattern (Figure 4), suggesting better model fit.

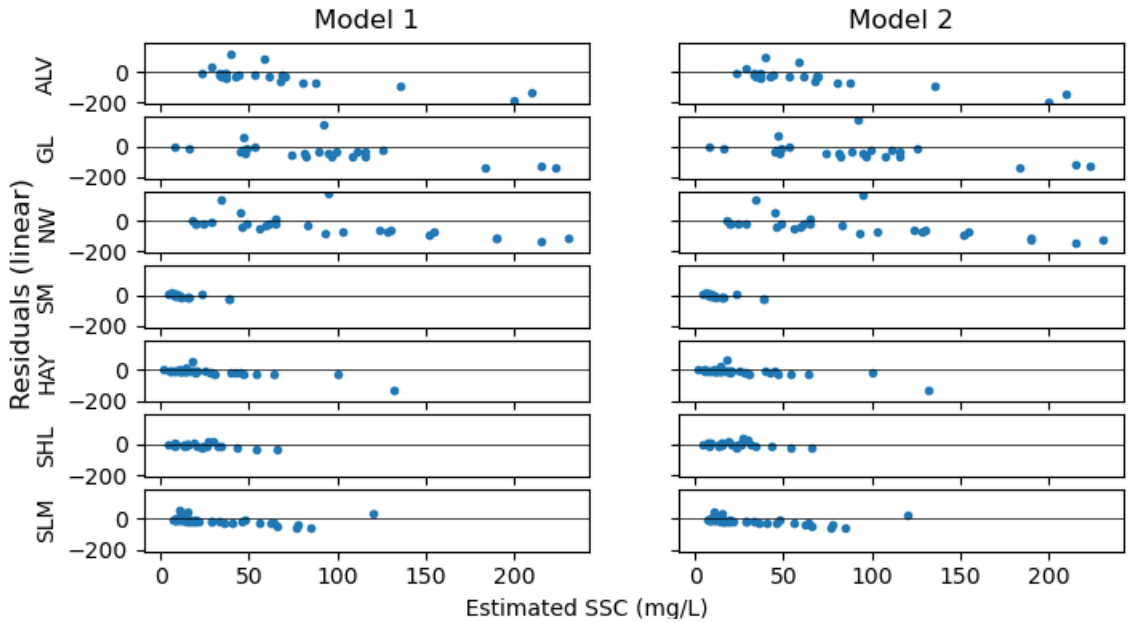

Figure 3. Residuals for linear (untransformed) slope-only Model 1 and Model 2. Residuals showed a linear pattern at several sites, with positive values at low SSC and negative values at higher SSC.

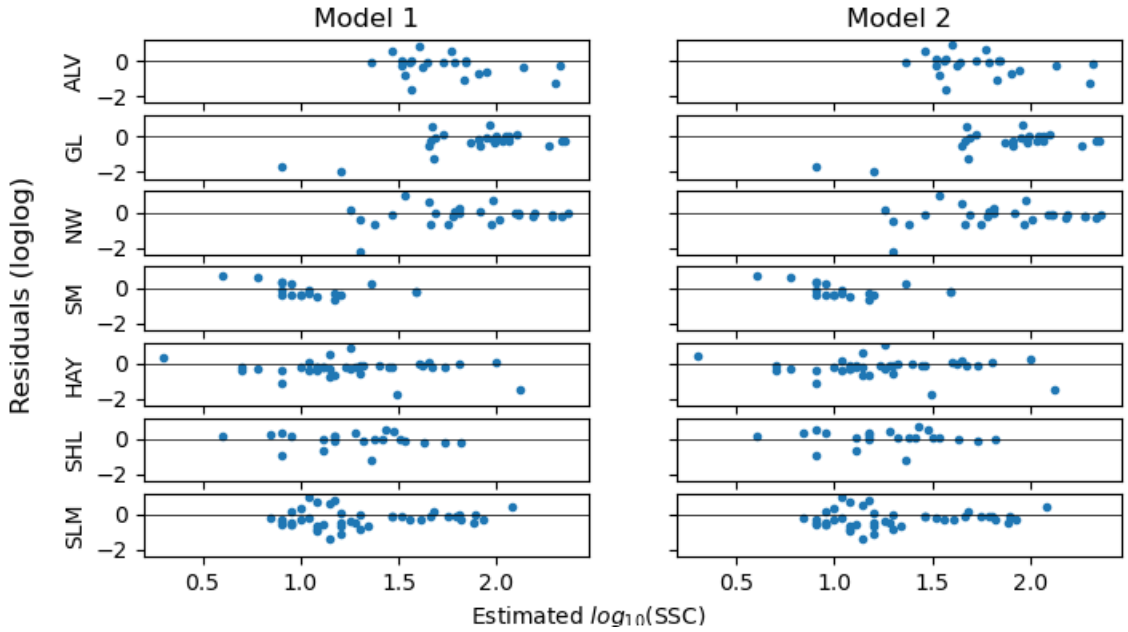

Figure 4. Residuals for log_{10}- log_{10} transformed slope-only Model 1 and Model 2. Residuals for log_{10}-log_{10} transformed models showed much more even spread than for models run on untransformed data.

In addition to model fit and residual analysis, another factor that was taken into consideration was the maximum turbidity that can be reliably used to estimate SSC. The USGS recommends against calculating SSC when turbidity > 110% the maximum value used during calibration. By grouping sites by habitat, the largest turbidity calibration value recorded by any site becomes the value used for all sites. Given that R^2 (Table 4), model coefficients (Table 6), and residuals (Figure 4) were similar between log_{10}-log_{10} transformed slope-only Model 1 and Model 2, this increase in maximum turbidity became the deciding factor when evaluating models. The model selected for final SSC calculation was Model 1: habitat-based LSLR, in slope-only form with log_{10}-log_{10} transformed data. The results from this final model for the 7 EXO2 sites are depicted in Figure 5. Results from the log_{10}-log_{10} slope-only LSLR used to calibrate EDL are presented in Figure 6.

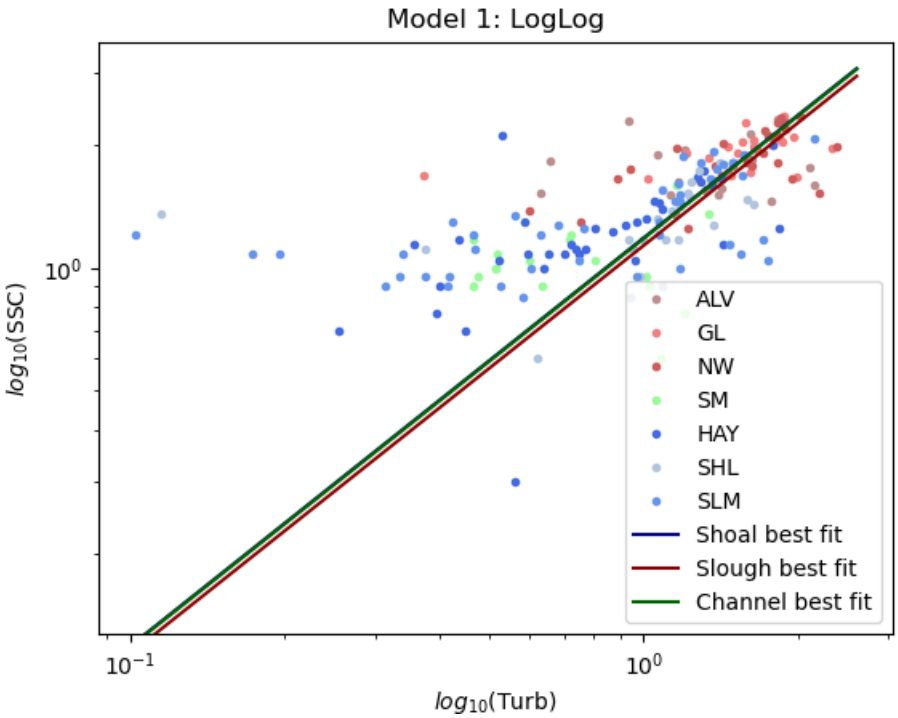

Figure 5. log_{10}(turb) vs. log_{10}(SSC) along with slope-only best fit lines from Model 1 (habitat-specific LSLR). Please note that shoal and channel best fits had very similar slopes (difference of <0.01), and so appear as the same line. Non-transformed turbidity values are FNU, non-transformed SSC are mg/L.

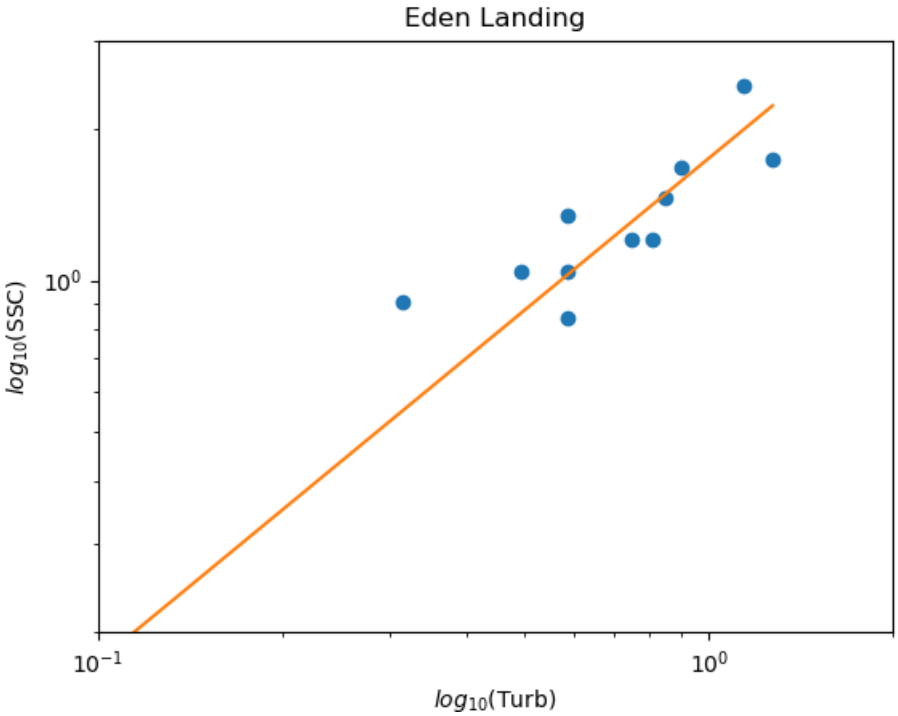

Figure 6. Slope-only log_{10}(turb) vs. log_{10}(SSC) at the Eden Landing station along with best fit line. Non-transformed turbidity values are NTU, non-transformed SSC are mg/L.

3.3 SSC Results

We generated estimates of continuous SSC by multiplying the retransformed values from Model 1 by the bias correction factor (BCF) described in Eq (7). Ideally the BCF is close to 1, implying strong correlations between SSC and turbidity and minimal correction needed during retransformation of $\log_{10}$ values (Rasmussen et al. 2009). The BCF at the 8 sites, including EDL, ranged from 0.91-1.30, suggesting strong model fit.

Final SSC datasets are nearly continuous for each station, although they contain some gaps during periods when the turbidity sensors were fouled or otherwise experienced malfunction such as loss of battery. Representative SSC data for 2023 from the 3 habitats are shown in Figure 7, with example gaps depicted. Due to site accessibility restraints, field servicing of turbidity monitoring stations typically occurs during floods tides when conditions are safest to access sites. As turbidity tends to be elevated during ebb tides and lower during flood tides, discrete SSC samples collected each servicing trip often do not capture peak values (e.g., Figure 2). Given these limitations, the turbidity thresholds for the habitat specific LSLR (Model 1) are 74, 268, and 153 FNU for the channel, slough, and shoal sites respectively, and 26 NTU for the EDL LSLR. This particularly low threshold at the EDL site is attributed to a site-specific LSLR based on only 14 discrete SSC samples. As a result, SSC results are only in range for calibration at EDL during 31% of the dataset. In contrast, turbidity data at the 7 EXO2 sites were within range for SSC calibration for 91-99% of the dataset.

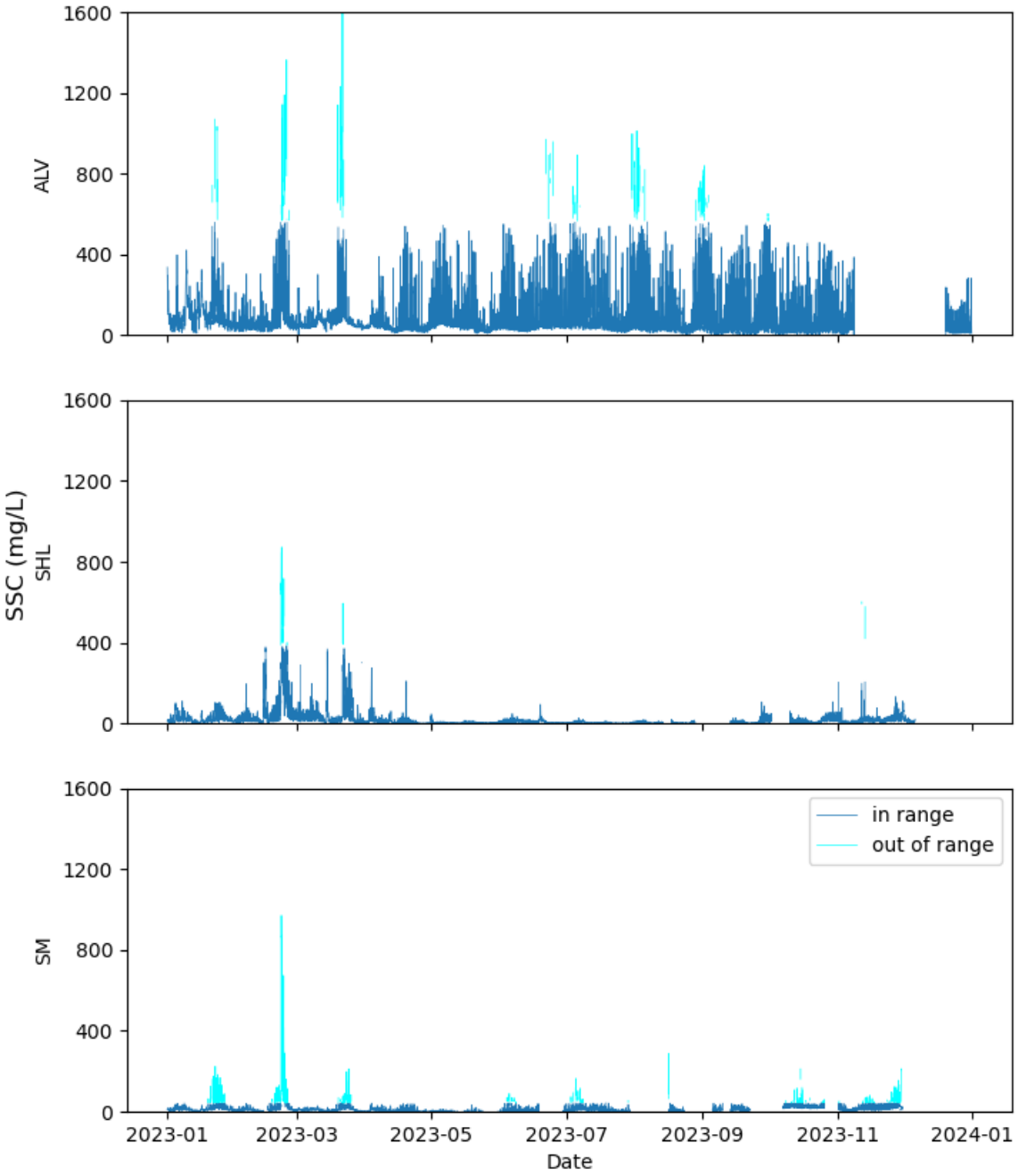

Figure 7. Representative time series of continuous SSC calculated from 2023 turbidity data at representative slough (ALV), shoal (SHL), and channel (SM) sites.

A slope-only Model 1 with $\log_{10}$-$\log_{10}$ transformation of data showed the strongest fit and best residuals, and was chosen as the final model for SSC calibration. However, we want to acknowledge that the choice of model and transformation has a substantial impact on final SSC estimates. Figure 7 compares SSC results between linear and transformed data using the slope-only Model 1 at 3 representative sites. In all cases, the $\log_{10}$-$\log_{10}$ fits are higher than linear ones. The higher the turbidity, the larger the gap in

estimated SSC between linear and log_{10}-log_{10} models. This discrepancy is particularly relevant at the slough sites, which have far higher turbidity than the shoal or channel sites.

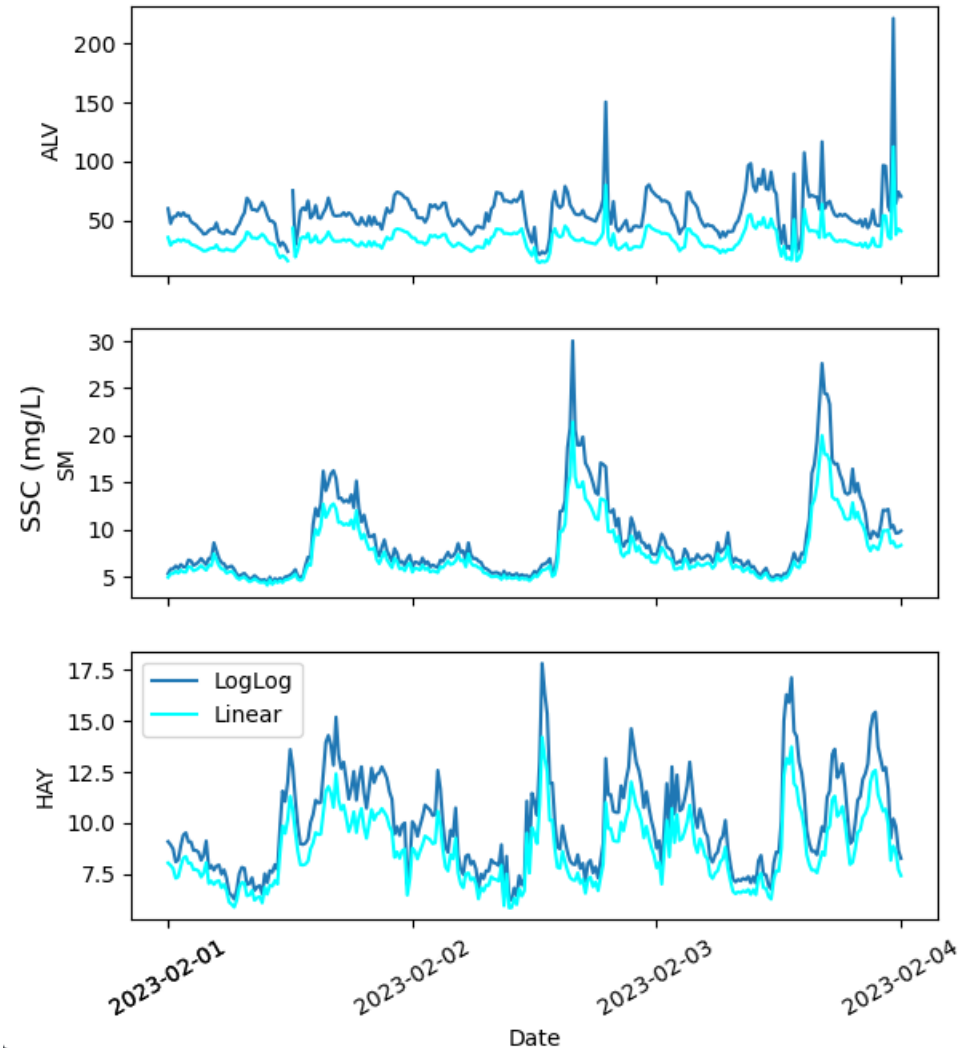

Figure 8. Representative time series of continuous SSC calculated from 2023 turbidity data at representative slough (NW), shoal (SHL), and channel (SM) sites. Note the y-axis range differs for each panel.

3.4 Wave results and statistics

The wave gauge was deployed at Hayward station (HAY), which is located on the exposed eastern shoal of South San Francisco Bay (Figure 1) and experiences windy conditions marked by substantial waves. During the Jan 2022-Oct 2024 sensor deployment, mean significant wave height and period were 0.14 m and 3.0 s, respectively, with interquartile ranges of 0.02-0.23 m and 2.4-3.2 s (Figure 9, Table 6). Wave periods were consistent with wind-driven waves (Hansen and Reidenbach, 2013), and in fact, wind speed data from the nearest California Irrigation Management Information System (CIMIS) station (171 – Union City) show that higher windspeeds were correlated with greater significant wave heights (Figure

10A). Greater significant wave height was in turn associated with higher mean turbidity (Figure 10B), likely due to wave-driven resuspension of benthic sediments and other particulates. An example of this effect is shown in Figure 11, where from January through March 2023 all elevated turbidity events occurred during periods of elevated wave height, particularly when wave height was > 0.45 m. Interestingly, despite mean turbidity increasing with mean significant wave height, the 99th percentile values of turbidity actually decreased with wave activity (Figure 10B). Taken together, these results suggest that although wind-driven waves likely enhance turbidity through benthic resuspension, this effect occurs against a backdrop of complicated tidal dynamics.

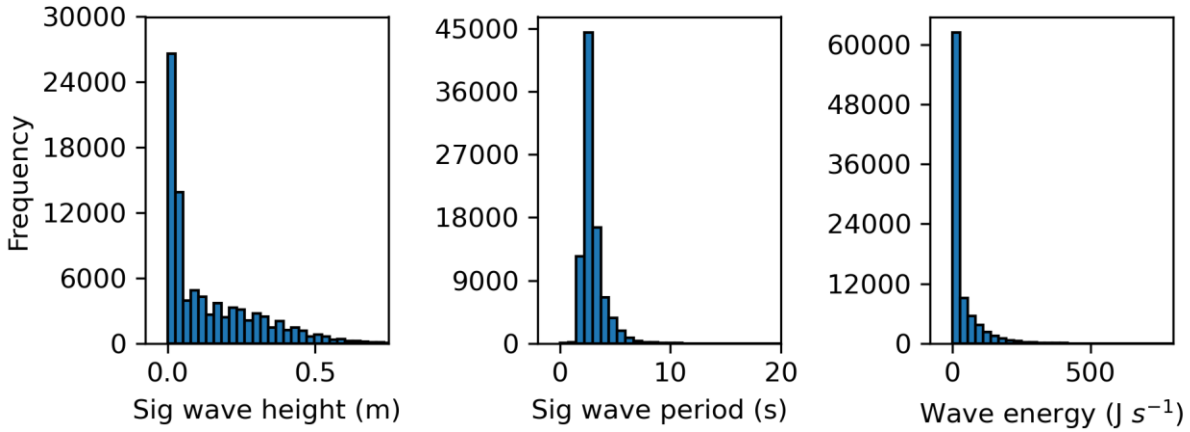

Figure 9. Histograms of relevant wave statistics at HAY station on eastern shoal of SB. Waves on the shoal tend to be wind-driven and have relatively low wave height and energy. However, during storm events waves as high as 1.3 m were measured over the shoal, resulting in substantial resuspension of benthic sediments.

Table 6. Summary of wave parameters measured at HAY mooring on the eastern shoal of SB.

Parameter	Mean	SD	P25th	P50th	P75th	Max
Sig wave height (m)	0.14	0.16	0.02	0.07	0.23	1.31
Sig wave period (s)	3.0	1.0	2.4	2.8	3.2	37
Wave energy (J m^{-2})	29	54	0.29	3.4	36	1400

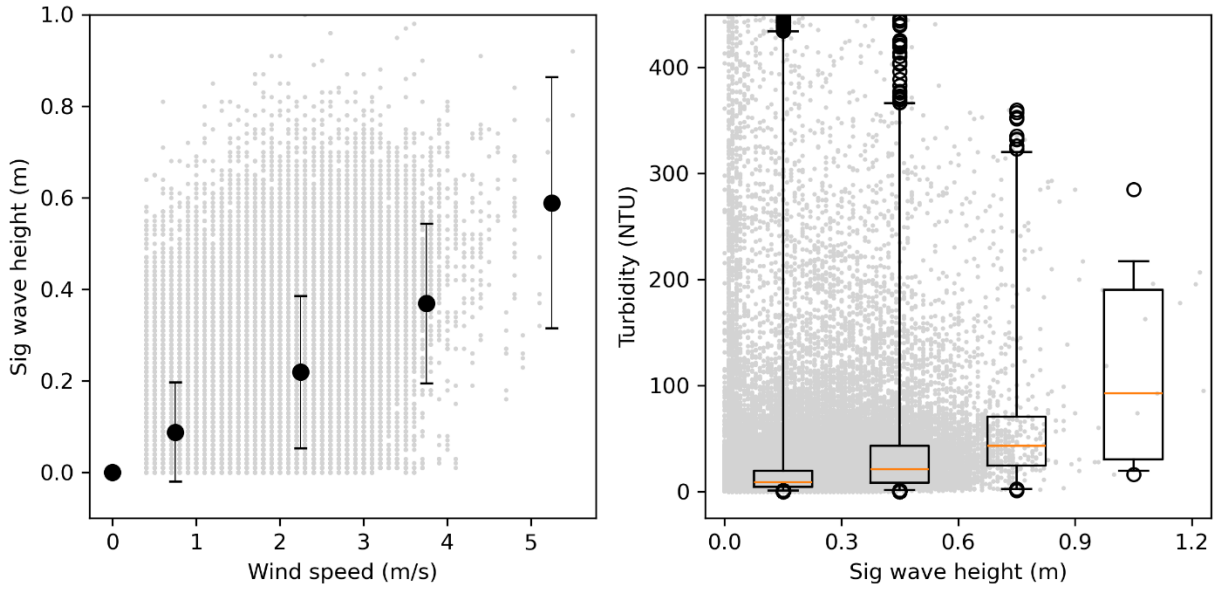

Figure 10. (A) Impact of wind speed (taken from CIMIS database) on significant wave height, and (B) impact of significant wave height on turbidity. Black circles in (A) represent the averages from 1 m/s windspeed bins ± SD. The boxes in (B) show the interquartile range and the whiskers show the 1-99th percentiles from 0.3 m sig wave height bins. In both panels grey dots represent instantaneous 15 min values. Wave height increased with windspeed at the HAY station, tending to result in higher turbidity due to resuspension of benthic sediments. Although low wave conditions had the lowest mean turbidity, they also showed the greatest spread between 1st and 99th percentiles, and accounted for the highest turbidity values measured during the study period.

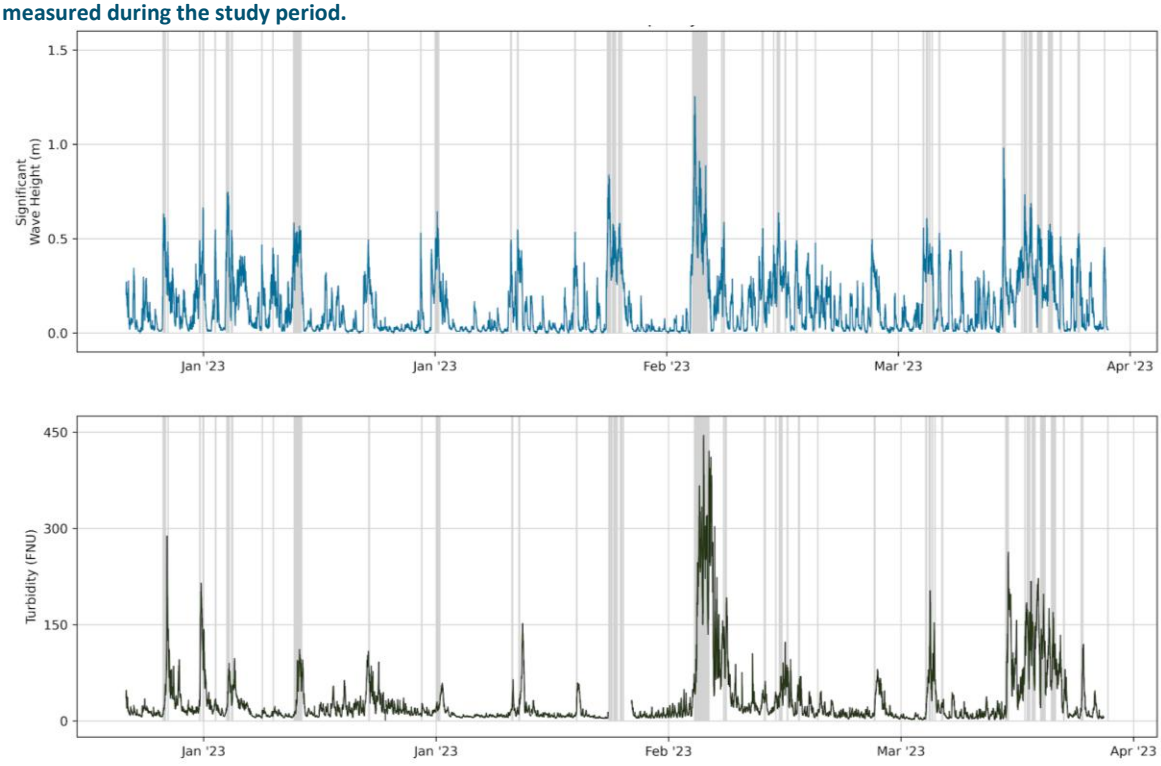

Figure 11. Example time series showing the impact of storm events on wave-driven resuspension of benthic sediments. The shaded areas indicate time periods when the significant wave height reached or exceeded 0.45 m, with these periods associated with substantial increases in turbidity.

5. Discussion

The goal of this project was to establish a robust turbidity-SSC calibration for SFB. Three models were evaluated at 7 EXO2 sites: 1) a set of 3 LSLRs based on the predominant subtidal habitats of SB and LSB, 2) a set of 7 site-specific LSLRs, and 3) a LMM. For all three models both linear and log_{10}-log_{10} data transformations were considered, and for Model 1 and Model 2 regressions were evaluated both with and without y-intercepts. The final calibration that was selected was Model 1, a set of habitat-based LSLRs, in slope-only form (no y-intercept) and with log_{10}-log_{10} transformed data. Model 1 was selected over Model 2 because grouping sites by habitat results in a larger number of samples per calibration and thus a higher threshold for which the turbidity-SSC calibration can be reliably applied. The USGS recommends caution when applying a turbidity-SSC calibration to values above 110% of the maximum used during calibration, and it is beneficial for SSC studies that this threshold be as high as possible.

Log_{10}-log_{10} transformation of data was selected as it resulted in substantially higher R^2 than untransformed data (Table 4), and showed more evenly dispersed residuals (Figure 3, Figure 4). Likewise, slope-only was chosen over an intercept model as it also had considerably greater R^2 (Table 4), and was more accurate at low turbidity values. When included, y-intercepts were high at all sites, particularly at the sloughs where they ranged from 65-70 mg/L (Table 5). Conceptually SSC must be 0 when turbidity is 0, as by definition the presence of suspended sediments results in positive turbidity. Substantial y-intercepts therefore bias SSC estimates for low values of turbidity, acting as a lower limit of SSC estimates. In other words, SSC estimated from intercept models at the slough sites cannot drop below 65-70 mg/L even when turbidity = 0. This final calibration model represents a change from the preliminary Year 1 and Year 2 reports, which utilized an LMM. This change was made because the LMM failed to converge when the y-intercept was removed.

Our calibration results differ somewhat from past USGS turbidity-SSC calibrations for SFB, despite both using LSLRs. The USGS calibration for the Dumbarton Bridge (DMB), the only USGS station in the South Bay, is a slope + intercept LSLR with linear data, and takes the form: $SSC_{DMB} = 1.68 * turb_{DMB} + 7.92$ (Livsey and Downing-Kunz 2020). This type of calibration differs our final slope-only log_{10}-log_{10} model, which for the channel site was $SSC_{chan} = 10^{1.18*log_{10}(turb)} * 1.2$ (Table 6). In our study, the equivalent slope + intercept untransformed model for the channel site was: $SSC_{chan} = 0.76 * turb_{chan} + 7.6$ (Table 5), which has a slope approximately half of the USGS calibration. Applying these three calibrations to turbidity data from our channel site (SM) shows how they result in different estimates of SSC (Figure 12). These discrepancies likely arise from site differences between SM and DMB, as well as from the use of different instruments for turbidity data collection (USGS - YSI 9520, this study – YSI EXO2). Nevertheless, these differences highlight the importance of continued SSC monitoring and refinement of turbidity-SSC relationships to ensure accurate calibrations.

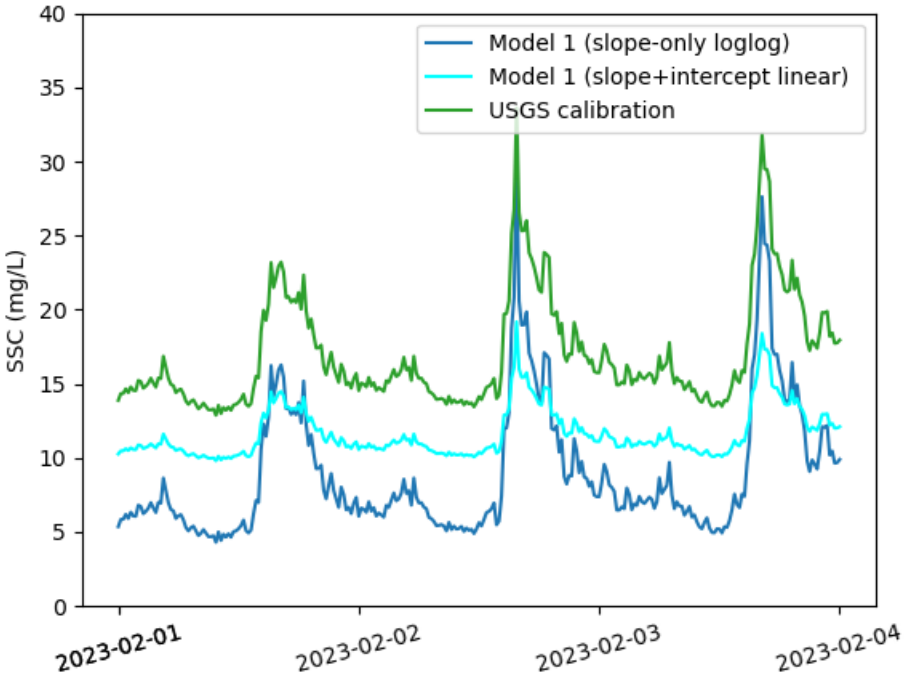

Figure 12. Comparison of estimated SSC at the SM station calculated using our final calibration model (slope-only $log_{10}log_{10}$) vs. SSC calculated using a USGS calibration defined at the Dumbarton Bridge (Figure 1). As the USGS calibration relies on a slope + intercept LSLR, results from the equivalent model in our study are also shown. SSC estimated using the USGS relationship was somewhat different from that estimated using our final calibration, which may be due to differences between sites and instruments used for turbidity data collection.

Both turbidity and SSC showed clear spatial patterns in SFB, with higher values in the sloughs than the shoal or deep channel (Table 2, Table 3). ALV and GL are connected to a complex network of former salt ponds, several of which are in the process of restoration (SFEI, 2016), and NW drains a salt marsh (Figure 1), resulting in consistently elevated SSC for all slough sites with little seasonal variability (Figure 2, Figure 7). The shoals demonstrated a different pattern, with mostly low turbidity and SSC punctuated by periods of elevated levels from wave-driven resuspension of benthic sediments. Our wave gauge at HAY demonstrated increased wave height with windspeed, and increased turbidity with wave height (Figure 10). As a result, we were able to identify storms as a major driver of increased turbidity and SSC in the region (Figure 11).

This effort has resulted in the most comprehensive SSC dataset that exists for San Francisco Bay, with high-frequency data spanning 8 locations and 3 years. Although this report focuses on the time period from 2021-2024, the underlying turbidity datasets stretch back as far as 2013 at some stations, and MSP data collection remains ongoing. Our hope is that this rich dataset will be used for future, more detailed studies of sediment dynamics in SFB, such as estimating sediment transport through the deep channel of the Bay, quantifying sediment delivery to the SB shoals, or estimating marsh erosion and/or accretion in the slough-connected LSB marshes. The MSP dataset is a powerful tool, and by adding a SSC calibration to the MSP turbidity data collection, we can better understand and manage sediments in SFB.

NOTE: Turbidity data quality and future addendum

Please note that all MSP data, including the turbidity data used in this report, are currently undergoing refinements to QA/QC procedures. During this transition, the MSP team discovered an issue where erroneous data were not always correctly removed from the dataset. This removal issue primarily affects brief, substantial spikes in EXO2 measurements. Longer-term removals of data, such as days-long periods of instrument fouling, are still captured correctly. Examples of erroneous spikes in turbidity data, which previously had been removed, are visible in Figure 2 and Figure 7. Given the transient nature of these spikes, they are unlikely to substantially affect the results of this report, including summary turbidity statistics (Table 2). Additionally, we closely examined the specific turbidity data used to create SSC calibrations (Figure 5), finding these data to be valid. Nevertheless, we plan to submit an addendum to this report including updated results and figures once this removal issue is resolved. The projected timeline is 2-3 months.

6. Project data repository

Data for this report will be available for download from the SFEI website once the underlying MSP data issue is resolved. The data that will be available are described in Table 7, and include summaries of discrete SSC samples, wave gauge measurements, turbidity measurements, and continuous SSC estimates.

Table 7. Directory for project data repository.

File Name	Contents	Years
discrete_sediment.csv	• Total sediment (g) • Sediment concentration (mg/L) • Total sand (g) • Total fine (g) • Percent finer (%)	2020-2024
turbidity_ssc.csv	• Continuous turbidity (FNU or NTU) • Continuous suspended sediment concentration (mg/L)	2022-2024
wave.csv	• Water column depth (m) • Significant wave height (m) • Significant wave period (s) • 90 percentile wave height (m) • 90 percentile wave period (s) • Maximum wave height (m) • Maximum wave period (s) • Average wave height (m) • Average wave period (s) • Wave energy (J/m^2) • Pressure (dbar) • Sensor depth (m)	2022-2024

7. References

Cloern, J.E., (1987), Turbidity as a control on phytoplankton biomass and productivity in estuaries: Continental Shelf Research, v. 7, no. 11/12, p. 1367–1381.

Cloern, J. E., and Jassby, A.D., (2012), Drivers of change in estuarine-coastal ecosystems: Discoveries from four decades of study in San Francisco Bay, Rev. Geophys., 50, RG4001, doi:10.1029/2012RG000397

Hansen, J.C.R., and Reidenbach M.A., (2013), Seasonal growth and senescence of a Zostera marina seagrass meadow alters wave-dominated flow and sediment suspension within a coastal bay, Estuaries and Coasts, 36, 1099-1114

Livsey, D., and Downing-Kunz, M., (2020), A summary of water-quality monitoring in San Francisco Bay in water year 2017: U.S. Geological Survey Scientific Investigations Report 2020–5064, 78 p., https://doi.org/10.3133/sir20205064.

Marvin-DiPasquale, M., Slotton, D., Ackerman, J.T., Downing-Kunz, M., Jaffe, B.E., Foxgrover, A.C., Achete, F., and van der Wegen, M., (2022), South San Francisco Bay Salt Pond Restoration Project—A synthesis of Phase-1 mercury studies, U.S. Geological Survey Scientific Investigations Report 2022-5113, 147 p., https://doi.org/10.3133/sir20225113.

Mourier, L., Volaric, M., Chelsky, A., Senn, D.B., (2023), Continuous Suspended Sediment Monitoring in South and Lower South San Francisco Bay Year One Report for 2022. SFEI Contribution No. 1135. San Francisco Estuary Institute: Richmond, CA

Mourier, L., Montgomery, L., Volaric, M., Chelsky, A., Senn, D.B., (2024), Continuous Suspended Sediment Monitoring in South and Lower South San Francisco Bay Year Two (2023) Report. SFEI Contribution No. 1188. San Francisco Estuary Institute: Richmond, CA.

Newcombe, C. P., and Jensen, J. O.T., (1996), Channel Suspended Sediment and Fisheries: A Synthesis for Quantitative Assessment of Risk and Impact, North American Journal of Fisheries Management, 16:4, 693-727

Rasmussen, P.P., Gray, J.R., Glysson, G.D., and Ziegler, A.C., (2009), Guidelines and procedures for computing time-series suspended-sediment concentrations and loads from in-stream turbidity-sensor and streamflow data: U.S. Geological Survey Techniques and Methods, book 3, chap. C4, 52 p.

SFEI, (2016), Lower South Bay Nutrient Synthesis. San Francisco Estuary Institute, Richmond. CA. Contribution #barger, G.G., Wright, S.A., and Schoellhamer, D.H., (2013), A sediment budget for the southern reach in San Francisco Bay, CA: implications for habitat restoration: Marine Geology, v. 345, p. 281-293.

Valoppi, L., (2018), Phase 1 studies summary of major findings of the South Bay Salt Pond Restoration Project, South San Francisco Bay, California. US Geological Survey Open-File Report 2018–1039, 58 p., https://doi.org/10.3133/ofr20181039